How Isolated Are the Electronic States of the Core in Core/Shell Nanoparticles?

Zuoti Xie,[†] Tal Z. Markus,[†] Gilad Gotesman,[†] Zvicka Deutsch,[‡] Dan Oron,[‡] and Ron Naaman*,[†]

[†]Department of Chemical Physics, Weizmann Institute of Science, Rehovot 76100, Israel, and [‡]Department of Physics of Complex Systems, Weizmann Institute of Science, Rehovot 76100, Israel

ABSTRACT We investigated how isolated are the electronic states of the core in a core–shell (c/s) nanoparticles (NPs) from the surface, when the particles are self-assembled on Au substrates *via* a dithiol (DT) organic linker. Applying photoemission spectroscopy the electronic states of CdSe core only and CdSe/ZnS c/s NPs were compared. The results indicate that in the c/s NPs the HOMO interacts strongly with electronic states in the Au substrate and is pinned at the same energies, relative to the Fermi level, as the core only NPs. When the capping molecules of the NPs were replaced with thiolated molecules, an interaction between the thiol groups and the electronic states of the NPs was observed that depends on the properties of the NPs studied. Thiols binding to the NPs induce the formation of surface trap states. However, while for the core only CdSe NPs the LUMO states are strongly coupled to the surface traps, independent of their size, this coupling is size dependent in the case of the CdSe/ZnS c/s NPs. For a large core, the LUMO is decoupled from the surface trap states. When the core is small enough, the LUMO is delocalized and interacts with these states.

KEYWORDS: photoelectron spectroscopy · electronic structures · core/shell nanoparticles · electronic wave function · surface trap states

Semiconductor nanoparticles (NPs) exhibit interesting size-tunable optical properties due to the confinement of the electronic wave functions.[1−3] The high surface-to-volume ratio of small NPs suggests that the surface affects significantly their structural and electronic properties. Indeed surfaces capped by organic or inorganic layers strongly influence the emission efficiency of the NPs.[2−8] By producing a core, made of one semiconductor material, and coating it with a shell made from another material, the electronic properties of this core–shell (c/s) NP can be engineered, and predesigned electronic properties are obtained.[2,3,7−12] Such c/s NPs as CdSe core-capped with wider bandgap ZnS shell form type I c/s NPs which have improved optical properties as compared to those of the CdSe core-only NPs.[2,3] The improvement is a result of the confined potential of the excited electron–hole pair which reduces their interaction with traps on the surface and the environment. This confinement can be tuned by varying the shell properties (material and thickness) and/or the radius of the core.[9,10,13−15] For many applications the positions of the occupied and unoccupied orbitals of the NPs are highly important, specifically the question of how their energies can be controlled by modifying the surface properties.[15−18]

In the present work we address the question to what extent are the energy states of the core isolated from the surface in a c/s NP and what properties of the NP affect this insulation. We present results on the electronic structures of CdSe core-only and CdSe/ZnS c/s NPs self-assembled as monolayers on Au by an organic linker. In these NPs the HOMO and the LUMO are of $1S_{3/2}$ and $1S_e$ symmetry, respectively. The results obtained by low-energy photoelectron transmission (LEPET) spectroscopy[18,19] (see Scheme 1) indicate that the highest occupied molecular orbitals (HOMOs) of CdSe/ZnS c/s NPs and the CdSe core-only NPs are located at the same energy and are pinned relative to the Fermi level of the Au substrate. Applying two-photon photoelectron (TPPE) spectroscopy[18,19] (see Scheme 1) we observed the lowest unoccupied molecular orbitals (LUMOs) of both the core and of the shell. Organic molecules that bind to the NPs *via* thiol groups were used for introducing surface trap states. It was found that, while the LUMOs in the core-only CdSe NPs are strongly coupled to the surface traps, this coupling is size dependent in the case of the CdSe/ZnS c/s NPs. For a large core, the LUMO is localized almost entirely in the core, and there is no significant coupling with the surface trap states. However, when the core is small enough, the LUMO is delocalized and penetrates into the shell, thus interacting with the surface trap states.

RESULTS AND DISCUSSION

Scheme 1 presents the two photoemission techniques applied in the current study

*Address correspondence to ron.naaman@weizmann.ac.il.

Received for review August 11, 2010 and accepted December 23, 2010

Published online January 05, 2011
10.1021/nn102002x

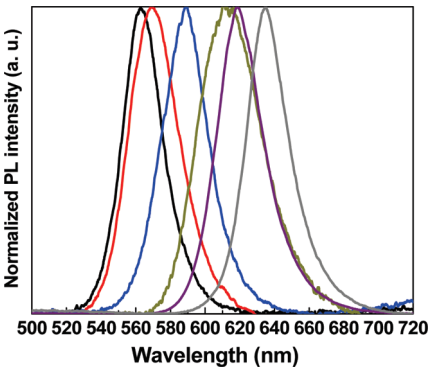

Figure 1. Photoluminescence signals (λ_{ex} = 457 nm) obtained for four differently sized CdSe and two differently sized CdSe/ZnS NPs whose monolayers are adsorbed to Au substrates through an organic linker. It shows the CdSe/ZnS 3.8 nm, CdSe 3.3 nm, CdSe 3.7 nm, CdSe 4.7 nm, CdSe/ZnS 5.8 nm, and CdSe 6 nm maximum emission at 562 nm (black), 569 nm (red), 590 nm (blue), 612 nm (dark yellow), 618 nm (purple), and 635 nm (gray), respectively.

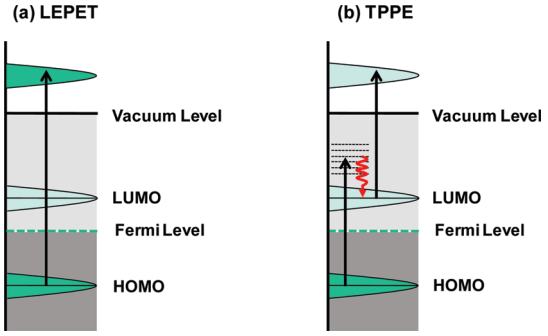

Scheme 1. The photoemission schemes[a]

[a] In the case of LEPET (a) electrons are ejected from below the Fermi level applying photon energy that exceeds the ionization potential of the nanoparticles. In the TPPE experiments (b), the electrons are ejected by a two-photon process in which the first photon excites the nanoparticles to unoccupied states located below the vacuum level. The excited electrons relax fast to the lowest unoccupied state (the LUMO) from which they are ejected by the second photon.

for determining the electronic states of the NPs adsorbed on the gold substrate. In the case of the LEPET method (Scheme 1a) electrons are ejected from below the Fermi level applying photon energy that exceeds the ionization potential of the nanoparticles. In the case of the TPPE experiments (Scheme 1b), the electrons are ejected by two-photon process in which the first photon excites the NPs to unoccupied states located below the vacuum level. The excited electrons relax rapidly to the lowest unoccupied state (the LUMO) from which they are ejected by the second photon.

Figure 1 presents the photoluminescence spectra of all the NPs studied when they are adsorbed on the gold substrate through the organic linker. Figure 2a shows the LEPET spectra from gold substrates coated with a monolayer of DT to which CdSe NPs were adsorbed at different adsorption times. By increasing

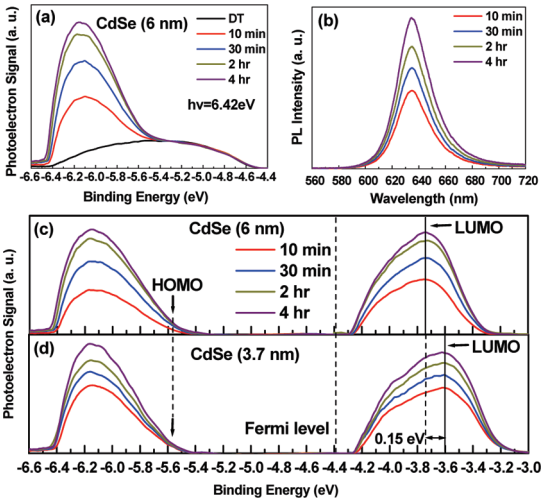

Figure 2. Results for different adsoption times of CdSe NPs on DT/Au from 10 min up to 4 h. (a) Normalized LEPET spectra. (b) PL of CdSe (6 nm). The difference LEPET spectra (below the Fermi level) that are obtained by subtracting the spectrum of the DT/Au, and TPPE spectra (above the Fermi level) of (c) CdSe (6 nm) and (d) CdSe (3.7 nm). The results show that the HOMO is pinned and the LUMO varies with NPs' sizes. The shifts observed correspond to an energy shift of ~0.15 eV between the NPs, which is consistent with the observed optical energy gap difference between the different NPs.

the adsorption time the NPs coverage is increased, as indicated also by the photoluminescence spectra presented in Figure 2b. In the LEPET spectra, the peak at a binding energy of about −6.2 eV is not present for samples that do not contain NPs, and this peak increases as the adsorption time increases from 10 min up to 4 h. There is a linear correlation between the intensities of this peak in the LEPET spectra and the intensities of the PL spectra (Supporting Information Figure S2), indicating that this peak stems from electrons ejected from the NPs. In Figure 2c,d the LEPET spectra are shown after subtraction of the gold-coated DT spectrum (with no NPs). Since the LEPET spectra reflect the density of states below the Fermi level, the peak on the left in Figure 2c,d presents the HOMO of the CdSe NPs (two sizes of 6 and 3.7 nm)/DT/Au both starting at −1.20 ± 0.05 eV relative to the Fermi level. The results from the TPPE experiments are shown on the right side of Figure 2c,d and were obtained by using two photons from the same laser pulse, each photon energy being 4.28 eV. The peak appears only for samples containing NPs and increases as a function of adsorption time, indicating that it represents the LUMO of the NPs and is located at 0.65 ± 0.05 eV and 0.80 ± 0.05 eV above the Fermi level for the 6 and 3.7 nm diameter NPs, respectively. The peak position relative to the Fermi level was found to be the same, independent of the wavelength used. Here, the HOMO energy is defined by the cutoff in the LEPET spectra, while the LUMO is defined by the peak in the TPPE spectra.[18] The HOMO−LUMO energy gaps obtained

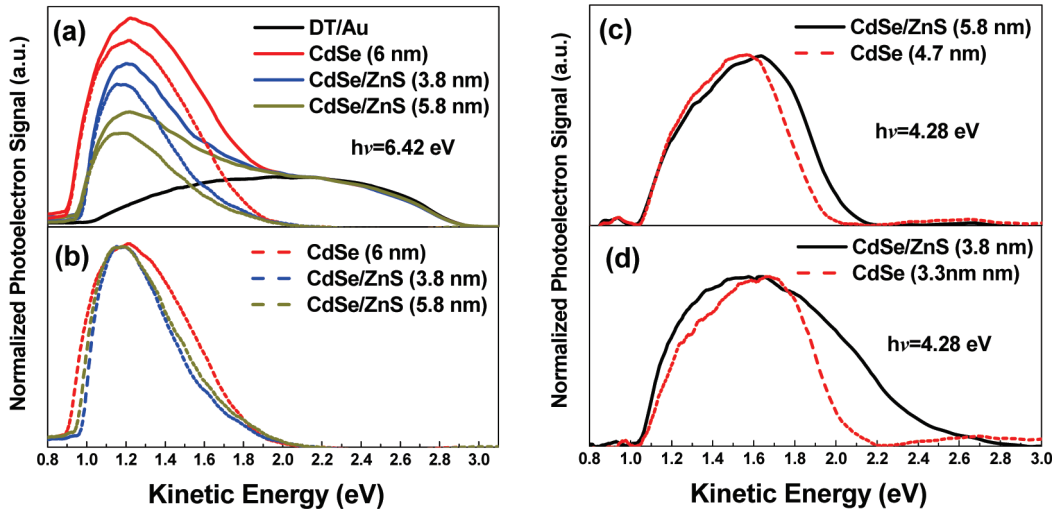

Figure 3. (a) Normalized LEPET spectra (solid lines) of DT/Au (black), CdSe 6 nm (red), c/s CdSe/ZnS 3.8 nm (blue), and c/s CdSe/ZnS 5.8 nm (dark yellow). The dashed lines show the difference LEPET spectra that are obtained by subtracting the spectrum of the DT/Au. It is clearly seen in the normalized difference spectra (b) that the HOMO is pinned even in the case of the core−shell NPs. (c) TPPE spectra of c/s CdSe/ZnS 5.8 nm (black solid line), CdSe 4.7 nm (red dashed line). (d) TPPE spectra of c/s CdSe/ZnS 3.8 nm, (black solid line), and CdSe 3.3 nm (red dashed line).

from the LEPET and TPPE spectra are 1.85 ± 0.10 eV and 2.00 ± 0.10 eV for the 6 and 3.7 nm NPs, respectively. These values are consistent with the 1.95 and 2.10 eV values obtained from the PL measurements. It is important to note that, for both sizes of NPs, the HOMO is at the same energy and only the LUMO is shifted according to the expected change in energy gap.

This observation is consistent with the results reported in refs 17 and 18, indicating that the HOMO of different sizes of CdSe NPs is pinned relative to the Fermi level of the system. The question we address here is what happens to the HOMO in the case of c/s NPs that are adsorbed on gold. Are the electronic states of the core really isolated from the environment? Figure 3a shows the LEPET spectra for the CdSe core-only and CdSe/ZnS c/s NPs. In all cases the HOMO is positioned at 1.20 ± 0.05 eV below the Fermi level. In the case of CdSe/ZnS c/s NPs the peak of the HOMO is somewhat narrower than that of the core only, indicating that there is no more than the single HOMO state, namely we do not observe the HOMO of the ZnS shell. This may be due to the ZnS HOMO being located at binding energies exceeding the photon energy of 6.42 eV.[13,20] This is consistent with the bulk properties of ZnS, in which the conduction band is located about 0.6 eV below that of CdSe.[21]

Since the PL spectra of the core-only 4.7 and 3.3 nm NPs are very similar to those of the c/s 5.8 and 3.8 nm, respectively, it is relevant to compare their TPPE spectra. The TPPE spectra of CdSe/ZnS c/s NPs are broader and show shifts to higher kinetic energies, as compared to those of the core-only NPs, as seen in Figure 3c and d. This broadening of the TPPE spectra could result from the contribution of states in the shell or on the surface. The red dashed curves in Figure 3c and 3d show that the LUMOs of the "core-only NPs" are located at 0.71 ± 0.05 eV and 0.87 ± 0.05 eV above the Fermi level for the 4.7 and 3.3 nm NPs, respectively. These results are consistent with the pinning of the HOMO. The LUMOs of the CdSe/ZnS (5.8 nm) and CdSe/ZnS (3.8 nm) c/s NPs are at 0.71 ± 0.05 eV and 0.91 ± 0.05 eV above the Fermi level, respectively, which is also consistent with the pinning of the HOMO.

It is expected that the electronic properties of NPs will be very sensitive to the details of the electronic wave functions[7−10,13−15,22−24] and therefore also to the existence of surface states.[2−6] Adsorption of thiols to NPs is known to induce the formation of trap states on the surface of the NPs.[5,6,25,26] This effect is observed by the thiol adsorption-induced quenching enhancement of the PL. For probing "how isolated is the core in a core−shell NP", we replaced the original capping of the NPs by readsorption of thiolated molecules, after the formation of the NPs monolayers on the DT/Au. We employed photoemission to probe how the formation of the surface states, caused by the thiol binding, affects the HOMO and LUMO in core only and c/s NPs. The series of sample studied included DT/Au, NPs/DT/Au, DT/NPs/DT/Au, for CdSe core only and CdSe/ZnS c/s NPs.

Figure 4 presents the PL, LEPET, and TPPE spectra of CdSe (6 nm) adsorbed through DT on Au, and the same sample after it was immersed in solution containing DT. In the latter case, DT was adsorbed on the NPs, and the sample is denoted as DT/CdSe (6 nm)/DT/Au. Figure 4a shows that PL of CdSe core only is quenched by ~90% following the adsorption of DT. This quenching is a result of a nonradiative decay pathway opened upon adsorption of the thiols and the formation of trap

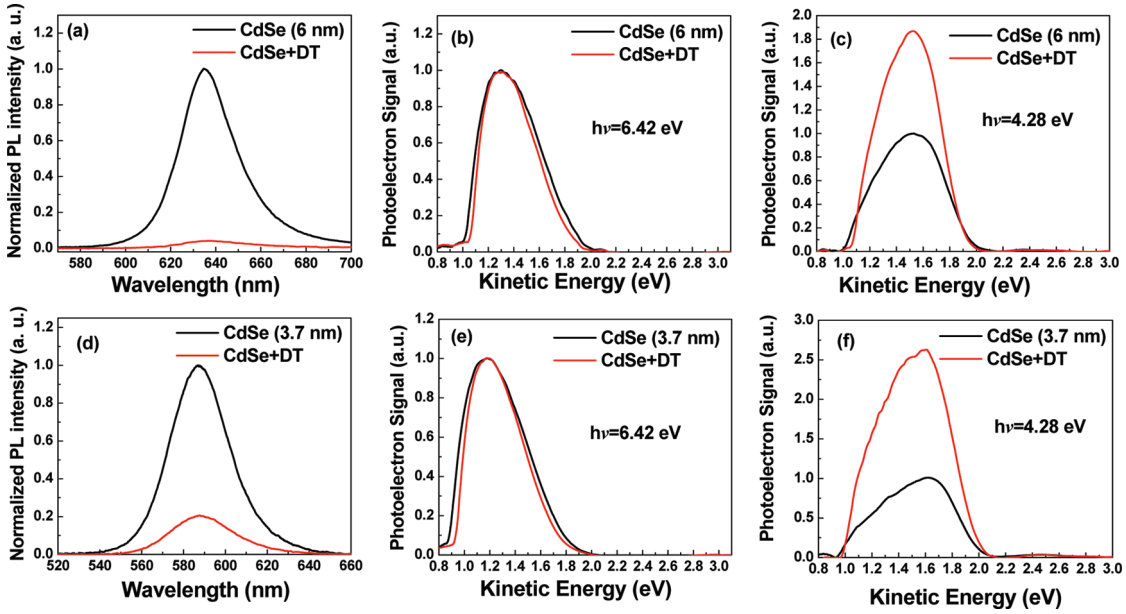

Figure 4. (a) PL spectra (b) difference LEPET spectra, and (c) TPPE spectra of CdSe (6 nm) and DT/CdSe (6 nm). (d) PL spectra (e) difference LEPET spectra, and (f) TPPE spectra of CdSe (3.7 nm) and DT/CdSe (3.7 nm).

states. Since all photoemission experiments were performed with the same laser intensity, we could subtract the signal resulting from the DT/Au substrate from the LEPET spectra of the sample with the NPs, and the results are shown in Figure 4b. The intensity of the HOMO of CdSe core only is not affected by the adsorption of the DT. However, in the TPPE results (Figure 4c) the adsorption of DT causes a significant increase in the intensity of the LUMO of the core-only NPs. Since the TPPE signal is proportional to the time-averaged population during the laser pulse, this dramatic increase in the intensity is a result of the excited electrons being transferred to longer-lived surface state traps, a process that lengthens their lifetime; as a result, the excited-state population increases, and so does the TPPE signal. This effect is supposed to decrease the PL lifetime of the excited NPs, as indeed was observed[27] consistent with the electron trap states formed on the surface of CdSe core-only NPs when changing their capping to a capping with thiolated molecules.[26] The unchanged intensities of the HOMO, upon adsorbing DT, can be explained by a relatively fast refilling time of electrons from the metal substrate back to the HOMO. This refilling is enhanced by the fact that, once electrons are ejected from the NPs by the LEPET process, the NPs are positively charged, and the positive potential drives a fast electron transfer from the substrate back to the layer. The same effect was observed when DT molecules were adsorbed on the smaller core-only NPs (Figure 4d,e,f). While the HOMO signal from the small CdSe NPs (3.7 nm) is not affected by the DT adsorption (Figure 4e), the LUMO signal increased dramatically, and the effect is even larger than observed with the larger core-only CdSe (6 nm) NPs (Figure 4f). This larger effect can be attributed to the stronger coupling of the trap states to the LUMO in the case of the small particles.

The effect of thiol adsorption seems to be dramatically different when considering type I CdSe/ZnS c/s NPs. It was reported that in these NPs the electron and hole wave functions are both highly confined to the core.[2,3,9,10] Figure 5 shows the PL (a), LEPET (b), and TPPE (c) spectra of CdSe/ZnS (5.8 nm)/DT/Au before and after adsorption of DT on top of the NPs. The PL is quenched by only ~10% when DT is attached to the NPs. This negligible effect is expected when the electron−hole excitation of the CdSe is "isolated" from the environment by the ZnS shell. However, contrary to the case of core-only NPs, the adsorption of DT on the large c/s NPs decreases the intensity of the HOMO signal (Figure 5b) and does not affect the intensity of the LUMO signal (Figure 5c). The reduction in the HOMO signal is explained by the weak coupling to the metal, due to the presence of the ZnS shell, which results in a very slow refilling of the HOMO.

The fact that the intensities of the PL and TPPE signals are unchanged upon adsorption of the thiols means that the LUMO is isolated from the traps. Hence, all observations related to the large core indicate that the core is isolated from the environment. Despite being pinned, the HOMO is interacting more weakly with the metal substrate relative to the case of core only, and the LUMO is not interacting with the trap states on the surface of the NPs. It is expected that the size of the core will affect the properties of its wave function in a c/s NP.[18−21]

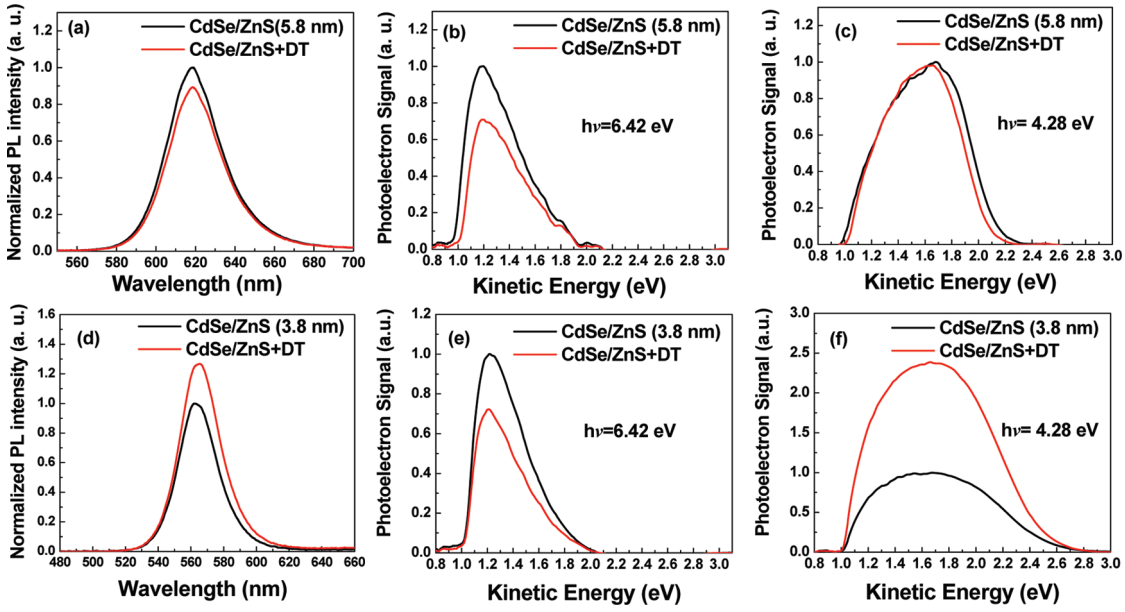

Figure 5. (a) The PL spectra, (b) difference LEPET spectra, and (c) TPPE spectra of CdSe/ZnS (5.8 nm) and DT/CdSe/ZnS (5.8 nm). (d) PL spectra, (e) difference LEPET spectra, and (f) TPPE spectra of CdSe/ZnS (3.8 nm) and DT/CdSe/ZnS (3.8 nm).

To investigate the size effect we used small CdSe/ZnS c/s NPs with an average diameter of 3.8 nm. Figure 5d shows the PL of these NPs on DT/Au and when DT molecules are adsorbed on the particles. For these particles, with a small core there is a small enhancement of the PL upon adsorption of the thiols on the NPs. The LEPET spectra in Figure 5e show the same changes resulting from the thiol bonding, as observed for the larger core (Figure 5b), namely the intensity of the HOMO is decreased when the DT molecules are adsorbed. This is again consistent with the HOMO being only slowly refilled when electrons are ejected from below the Fermi level by the UV photons. However, while for the larger particles the LUMO is not affected by the DT (Figure 5c), in the case of the smaller c/s particles, the intensity of the TPPE spectrum associated with the LUMO is increased by the DT adsorption. This increase results from excited electrons being transferred to surface traps. Namely, the density of states near the LUMO increases due to the adsorption of thiols, and therefore upon excitation more electrons are captured for a longer time. This causes the enhancement in the excited states' population during the laser excitation pulse. This is consistent with the observations in ref 3 that, in the case of the c/s CdSe/ZnS NPs with a smaller core, the leakage of excitons into the ZnS shell is pronounced. This enhancement of the LUMO, which indicate a strong coupling to trap states, is the same as observed in the core-only NPs (Figure 4c,f). Hence, for the smaller core in the CdSe/ZnS c/s NP, the LUMO is apparently delocalized, and its wave function is extended significantly into the shell.

CONCLUSIONS

The goal of the present study was to investigate to what extent are the electronic states of c/s NPs really isolated from the environment. This was done by PL measurements as well as by photoemission spectroscopy that probes the HOMO and LUMO of core-only and core−shell NPs adsorbed *via* an organic linker on a gold substrate.

The results indicate that the pinning of the HOMO relative to the Fermi level, observed before for core-only NPs, occurs also for type I c/s NPs. As a result, the change in the HOMO−LUMO gap, as a function of the NPs size, is expressed only by the change in the position of the LUMO relative to the Fermi level. Despite being pinned to the Au substrate, in the case of c/s NPs, the HOMO is coupled more weakly to the substrate and therefore, following photoexcitation and removing population from it, its refilling time is longer. Adsorption of thiols on the NPs causes the formation of traps states. The increased LUMO signal provides additional support to the formation of electron-trapping surface states. The coupling between the LUMO and those trap states is size dependent in the case of the c/s NPs, while this size dependence is not observed in the core-only NPs. Namely, while in the large CdSe/ZnS c/s NPs, the LUMO is confined within the core; in the case of the small CdSe/ZnS c/s the LUMO is delocalized and, as a result, interacts with the trap states on the surface created by the adsorbed thiols.

On the basis of our observations it is evident that assuming type I c/s NPs cores are isolated from the environment is crude. When NPs are adsorbed on a substrate with high density of states, such as metals, the

HOMO may be pinned to the substrate Fermi level even in c/s NPs. In addition, when the size of the core is small enough, the LUMO tends to extend into the shell and, as a result, becomes sensitive to the surface properties.

EXPERIMENTAL SECTION

The NPs/substrate assemblies consisted of CdSe (core only, capped with oleic acid, the detailed synthesis is described in ref 18) and CdSe/ZnS (type I c/s, Evident Technologies) NPs linked to a gold film by a monolayer of 1,9-nonanedithiol (DT). First, a DT monolayer was prepared on Au according to the procedures described in ref 28 by immersing a clean gold substrate in a methanol solution of 1 mM DT for 20 h. The samples were then rinsed with ethanol and dried with N_2. In order to attach the NPs, the DT self-assembled monolayer (SAM)-coated gold substrates (DT/Au) were immersed in a 0.5−10 μM solution of CdSe or CdSe/ZnS NPs in anhydrous toluene (99.8%, Aldrich). In this work six different NPs were used. Four different sizes of CdSe core-only NPs with an average diameter of 6, 4.7, 3.7, and 3.3 nm, maximum emissions at 635, 612, 590, and 569 nm, respectively, and two different sizes of CdSe/ZnS c/s NPs with an average diameter of 5.8 nm (maximum emission at 618 nm), and of 3.8 nm (maximum emission at 562 nm). After the adsorption of the NPs, the samples were rinsed and sonicated in toluene to remove any excess NPs that were not covalently attached and then dried by N_2 flow. In the core/shell NPs the shell thickness is about 1 nm.[29,30] In order to study how surface trap states affect the electronic structure of the NPs, the samples were further immersed in a solution of 1 mM DT in methanol for 1 h and then rinsed with ethanol and dried by N_2 flow. The samples were characterized by SEM (Supporting Information Figure S1) and by photoluminescence as shown in Figure 1. The desnity of the NPs is about 4000/μm^2. The details of the PL measurement setup were described elsewhere.[31] In the present work the NPs were excited by an argon ion laser at 457 nm.

The photoemission experiments were based on ejection of photoelectrons from the different NP assemblies in an ultrahigh vacuum chamber ($\leq 10^{-8}$ Torr). The experimental setup is similar to that described in refs 18, 19, and 32. The photoelectrons are emitted from the sample to the vacuum, where their energy is measured by a time-of-flight spectrometer. Because of the short lifetime of the electrons that are captured by the NPs and monolayer and because of the low laser intensity and repetition rate (10 Hz), the monolayer and the NPs are not charged by electrons between laser pulses. This was verified by observing a stable electron energy spectrum which does not vary with time.

In the LEPET process, electrons are excited by a laser pulse with photon energy higher than the work function of the sample. The photoelectrons are therefore emitted from states below the Fermi level to above the vacuum level and transmitted to the detector. This method provides information on the density of states of the system below the Fermi level, such as the HOMO.

In TPPE spectroscopy, photons with energy lower than the work function of the sample are used. The "pump" photons interact with electrons below the Fermi level and excite them to states above the Fermi level but below the vacuum level of the sample. If the laser pulses used are not very intense and are relatively long, the electrons excited by these first photons can relax either back to states below the Fermi level or to originally unoccupied states in the NPs monolayer. The second pulse of photons, the "probe" photons, also having energy below the work function of the substrate, are able to eject the electrons from these originally unoccupied states, to above the vacuum level. The measured kinetic energy of these photoelectrons provides information on their binding energy in these originally unoccupied states, namely on the LUMO of the monolayer. The energy scheme of the processes of LEPET and TPPE are shown in Scheme 1. In all of these studies, the samples were biased by −1 V versus the detector.

As is evident by the change in the workfunction as a result of attaching nanoparticles to the organic molecules, there is indeed charge transfer induced by the need to equilibrate the electrochemical potential on the substrate and in the nanoparticles. This shift is of about 0.2 to 0.3 eV, depending on the coverage of the nanoparticles. We can now easily calculate the charge that has been transferred and account for this shift by describing the layer of NPs as parallel capacitor. Assuming a dielectric constant of about 4 for the organic monolayer and a molecular length of 1.45 nm, we obtain a charge of about 3×10^{-17} coulombs per μm^2, namely about 200 electrons. The number of NPs per this area is about 4000 as extracted from the SEM image and therefore the amount of charge transferred from the NPs to the substrate per particle is about 0.05.

Acknowledgment. This work was partially supported by the U.S. DOE (Grant No. ER46430), by the Israel Science Foundation, and by the Grand Center. The electron microscopy studies were conducted at the Irving and Cherna Moskowitz Center for Nano and Bio-Nano Imaging at the Weizmann Institute of Science.

Supporting Information Available: This material is available free of charge *via* the Internet at http://pubs.acs.org.

REFERENCES AND NOTES

1. Alivisatos, A. P. Semiconductor Clusters, Nanocrystals, and Quantum Dots. *Science* **1996,** *271*, 933–937.
2. Hines, M. A.; Guyot-Sionnest, P. Synthesis and Characterization of Strongly Luminescing ZnS-Capped CdSe Nanocrystals. *J. Phys. Chem.* **1996,** *100*, 468–471.
3. Dabbousi, B. O.; Rodriguez-Viejo, J.; Mikulec, F. V.; Heine, J. R.; Mattoussi, H.; Ober, R.; Jensen, K. F.; Bawendi, M. G. (CdSe)ZnS Core−Shell Quantum Dots: Synthesis and Characterization of a Size Series of Highly Luminescent Nanocrystallites. *J. Phys. Chem. B* **1997,** *101*, 9463–9475.
4. Jones, M.; Lo, S. S.; Scholes, G. D. Quantitative Modeling of the Role of Surface Traps in CdSe/CdS/ZnS Nanocrystal Photoluminescence Decay Dynamics. *Proc. Natl. Acad. Sci. U.S.A.* **2009,** *106*, 3011–3016.
5. Liu, I. S.; Lo, H. H.; Chien, C. T.; Lin, Y. Y.; Chen, C. W.; Chen, Y. F.; Su, W. F.; Liou, S. C. Enhancing Photoluminescence Quenching and Photoelectric Properties of CdSe Quantum Dots with Hole Accepting Ligands. *J. Mater. Chem.* **2008,** *18*, 675–682.
6. Wuister, S. F.; Donega, C. M.; Meijerink, A. Influence of Thiol Capping on the Exciton Luminescence and Decay Kinetics of CdTe and CdSe Quantum Dots. *J. Phys. Chem. B* **2004,** *108*, 17393–17397.
7. Kim, S. J.; Fisher, B.; Eisler, H. J; Bawendi, M. Type-II Quantum Dots: CdTe/CdSe(Core/Shell) and CdSe/ZnTe-(Core/Shell) Heterostructures. *J. Am. Chem. Soc.* **2003,** *125*, 11466–11467.
8. Peng, X. G.; Schlamp, M. C.; Kadavanich, A. V.; Alivisatos, A. P. Epitaxial Growth of Highly Luminescent CdSe/CdS Core/Shell Nanocrystals with Photostability and Electronic Accessibility. *J. Am. Chem. Soc.* **1997,** *119*, 7019–7029.
9. Muller, J.; Lupton, J. M.; Lagoudakis, P. G.; Schindler, F.; Koeppe, R.; Rogach, A. L.; Feldmann, J.; Talapin, D. V.; Weller, H. Wave Function Engineering in Elongated Semiconductor Nanocrystals with Heterogeneous Carrier Confinement. *Nano Lett.* **2005,** *5*, 2044–2049.
10. Balet, L. P.; Ivanov, S. A.; Piryatinski, A.; Achermann, M.; Klimov, V. I. Inverted Core/Shell Nanocrystals Continuously Tunable Between Type-I and Type-II Localization Regimes. *Nano Lett.* **2004,** *4*, 1485–1488.
11. Talapin, D. V.; Koeppe, R.; Gotzinger, S.; Kornowski, A.; Lupton, J. M.; Rogach, A. L.; Benson, O.; Feldmann, J.;

Weller, H. Highly Emissive Colloidal CdSe/CdS Heterostructures of Mixed Dimensionality. *Nano Lett.* **2003,** *3*, 1677–1681.
12. Xie, R. G.; Kolb, U.; Li, J. X.; Basche, T.; Mews, A. Synthesis and Characterization of Highly Luminescent CdSe-Core $CdS/Zn_{0.5}Cd_{0.5}S/ZnS$ Multishell Nanocrystals. *J. Am. Chem. Soc.* **2005,** *127*, 7480–7488.
13. Haus, J. W.; Zhou, H. S.; Honma, I.; Komiyama, H. Quantum Confinement in Semiconductor Heterostructure Nanometer-Size Particles. *Phys. Rev. B* **1993,** *47*, 1359–1365.
14. Laheld, U. E. H.; Pedersen, F. B.; Hemmer, P. C. Exciton in Type-II Quantum Dots: Finite Offsets. *Phys. Rev. B* **1995,** *52*, 2697–2703.
15. Luo, Y.; Wang, L. W. Electronic Structures of the CdSe/CdS Core−Shell Nanorods. *ACS Nano* **2010,** *4*, 91–98.
16. Colvin, V. L.; Alivisatos, A. P.; Tobin, J. G. Valence-Band Photoemission from a Quantum-Dot System. *Phys. Rev. Lett.* **1991,** *66*, 2786–2789.
17. Carlson, B.; Leschkies, K.; Aydil, E. S.; Zhu, X. Y. Valence Band Alignment at Cadmium Selenide Quantum Dot and Zinc Oxide $(10\bar{1}0)$ Interfaces. *J. Phys. Chem. C* **2008,** *112*, 8419–8423.
18. Markus, T. Z.; Wu, M.; Wang, L.; Waldeck, D. H.; Oron, D.; Naaman, R. Electronic Structure of CdSe Nanoparticles Adsorbed on Au Electrodes by an Organic Linker: Fermi Level Pinning of the HOMO. *J. Phys. Chem. C* **2009,** *113*, 14200–14206.
19. Markus, T. Z.; Daube, S. S.; Naaman, R. Cooperative Effect in the Electronic Properties of Human Telomere Sequence. *J. Phys. Chem. B* **2010,** *114*, 13897–13903.
20. Nethercot, A. H. Prediction of Fermi Energies and Photoelectric Thresholds Based on Electronegativity Concepts. *Phys. Rev. Lett.* **1974,** *33*, 1088–1091.
21. Wei, S. H.; Zunger, A. Predicted Band-Gap Pressure Coefficients of All Diamond and Zinc-Blende Semiconductors: Chemical Trends. *Phys. Rev. B* **1999,** *60*, 5404–5411.
22. Barker, J. A.; Warburton, R. J.; O'Reilly, E. P. Electron and Hole Wave Functions in Self-Assembled Quantum Rings. *Phys. Rev. B* **2004,** *69*, 035327(1−9).
23. Brus, L. E. Electron-Electron and Electron-Hole Interactions in Small Semiconductor Crystallites: The Size Dependence of the Lowest Excited Electronic State. *J. Chem. Phys.* **1984,** *80*, 4403–4409.
24. Polland, H. J.; Schultheis, L.; Kuhl, J.; Gobel, E. O.; Tu, C. W. Lifetime Enhancement of Two-Dimensional Excitons by the Quantum-Confined Stark Effect. *Phys. Rev. Lett.* **1985,** *55*, 2610–2613.
25. Dorokhin, D.; Tomczak, N.; Velders, A. H.; Reinhoudt, D. N.; Vancso, G. J. Photoluminescence Quenching of CdSe/ZnS Quantum Dots by Molecular Ferrocene and Ferrocenyl Thiol Ligands. *J. Phys. Chem. C* **2009,** *113*, 18676–18680.
26. Baker, D. R.; Kamat, P. V. Tuning the Emission of CdSe Quantum Dots by Controlled Trap Enhancement. *Langmuir* **2010,** *26*, 11272–11276.
27. Gotesman, G.; Guliamov, R.; Oron, D.; Naaman, R. In preparation.
28. Aqua, T.; Cohen, H.; Vilan, A.; Naaman, R. Long-Range Substrate Effects on the Stability and Reactivity of Thiolated Self-Assembled Monolayers. *J. Phys. Chem. C* **2007,** *111*, 16313–16318.
29. Yu, W. W.; Qu, L. H.; Guo, W. Z.; Peng, X. G. Experimental Determination of the Extinction Coefficient of CdTe, CdSe, and CdS Nanocrystals. *Chem. Mater.* **2003,** *15*, 2854–2860.
30. Makhal, A.; Yan, H. D.; Lemmens, P.; Pal, S. K. Light Harvesting Semiconductor Core−Shell Nanocrystals: Ultrafast Charge Transport Dynamics of CdSe−ZnS Quantum Dots. *J. Phys. Chem. C* **2010,** *114*, 627–632.
31. Gotesman, G.; Naaman, R. Temperature-Dependent Coupling in Hybrid Structures of Nanoparticle Layers Linked by Organic Molecules. *J. Phys. Chem. Lett.* **2010,** *1*, 594–598.
32. Ray, S. G.; Daube, S. S.; Cohen, H.; Naaman, R. Electron Capturing by DNA. *Isr. J. Chem.* **2007,** *47*, 149–159.